Research Square

Preprints are preliminary reports that have not undergone peer review.
They should not be considered conclusive, used to inform clinical practice,
or referenced by the media as validated information.

Screening of Bacillus bacterial strains with capability of degrading T-2 toxin

Thanh Duy Nguyen
Griffith University
Yaoying Lu
Griffith University
Xiaojing Chen
Bioproton Pty Ltd
Linlin Ma
Griffith University
Yunjiang Feng
y.feng@griffith.edu.au

Griffith University

Article

Keywords: mycotoxins, T-2 toxin, HT-2 toxin, degradation, Bacillus, cytotoxicity

Posted Date: November 6th, 2026

DOI: https://doi.org/10.21203/rs.3.rs-10924385/v1

License: This work is licensed under a Creative Commons Attribution 4.0 International License.
Read Full License

Additional Declarations: Competing interest reported. Xiaojing Chen was employed by Bioproton Pty Ltd, Queensland, Australia.

Abstract

T-2 toxin (T-2) is a toxic fungal metabolite mainly produced by *Fusarium* species that are known to contaminate food products worldwide, posing serious risks to public health and the economy. Effective control of this toxin is therefore a key objective in food safety. Recent efforts to manage T-2 contamination have focused on utilizing microbes, especially bacterial species from the *Bacillus* genus, as promising toxin degraders. This study evaluated the *in vitro* capacity of ten *Bacillus* strains (BC1–10) in degrading T-2. Three out of ten strains demonstrated T-2 degradation activity, with complete toxin removal achieved within 96 hours under standard culture condition. The major biotransformation product of T-2 was isolated by high-performance liquid chromatography and structurally characterized by nuclear magnetic resonance spectroscopy as HT-2 toxin. Toxicity assessment in kidney-derived HEK293T cells showed that HT-2 was less toxic than T-2, with EC_{50} values of 12.8 and 1.8 nM, respectively. The findings supported the potential application of selected *Bacillus* strains as functional microbial additives to mitigate T-2 contamination and toxicity.

Introduction

T-2 toxin (T-2) is a notable member of the trichothecene mycotoxin family naturally produced by various fungal species of the genera *Fusarium*, *Myrothecium*, *Trichoderma*, *Trichothecium*, *Cephalosporium*, and *Stachyobotrys* (Chen et al. 2020; McCormick et al. 2011). This small molecule is commonly detected as a contaminant in foodstuff, such as wheat, rye, oats, rice, maize, and animal feeds, particularly in cooler and humid regions (Chen et al. 2020; Zhang et al. 2022). T-2 is highly toxic and, at the cellular level, can induce oxidative stress damage, disrupt mitochondrial functions, inhibit DNA and protein synthesis, and compromise cell membrane integrity (Cundliffe et al. 1974; Janik et al. 2021). In addition, this mycotoxin is readily absorbed from the gastrointestinal tract, and its ingestion and exposure have been associated with various adverse health conditions in animals such as hepatotoxicity, neurotoxicity, nephrotoxicity, immunotoxicity, and reproductive toxicity (Ihara et al. 1997; McCormick et al. 2011; Nayakwadi et al. 2020; Yang et al. 2019; Zhang et al. 2018). Therefore, effective management of T-2 contamination is of great interest to ensure food safety.

Strategies to decontaminate T-2, as well as other fungal toxins, have been investigated for several decades and can be categorized into physical, chemical, and biological approaches (Hamad et al. 2023; Luo et al. 2018). Physical methods involve techniques such as sorting, washing, and adsorption, to remove mycotoxins, while chemical approaches rely on chemical substances, like strong oxidizing or reducing agents, to destroy the toxins (Hamad et al. 2023; Luo et al. 2018; Yao et al. 2026). Although these techniques have been shown to reduce mycotoxins in food samples, they may compromise nutritional qualities or produce potentially harmful byproducts simultaneously (Adebo et al. 2021). In contrast, biological methods offer an alternative strategy through the use of microorganisms or enzymes to decompose fungal toxins biologically, providing advantages such as environmental compatibility, low cost, high efficiency, and specificity (Ji et al. 2016). Microbial decontamination of T-2 has been reported for a variety of microorganism genera such as *Wikerhamomyces*, *Rhodococcus, Eubacterium*, and

Blastobotrys (Fuchs et al. 2002; Garai et al. 2020; McCormick et al. 2012; Yang et al. 2025). Notably, accumulating evidence suggests that bacteria from the *Bacillus* genus are emerging as promising mycotoxin degraders owing to their resilience and high metabolic activity (Greco et al. 2025; Nguyen et al. 2024). Although *Bacillus* species are able to degrade several prevalent mycotoxins such as aflatoxins and zearalenone, limited information is available regarding their ability to metabolize T-2, with only a few studies addressing this topic in the literature (Hassan et al. 2021; Ma et al. 2023). Furthermore, existing studies on T-2 decontamination by *Bacillus* species have largely concentrated on overall toxin reduction, while the identity of the degradation products and their residual toxicity remain unclear (Chen et al. 2025; García-García et al. 2024). Constituently, the present study aims to provide further evidence supporting the ability of *Bacillus* bacteria in metabolizing T-2 by evaluating the *in vitro* T-2 biodegradation capacity of ten *Bacillus* strains (BC1 – 10). The biotransformation products of T-2, together with their toxicity on a mammalian cell line, were also investigated.

Materials and methods

Chemicals and reagents

Oxoid tryptone soya broth (TSB; Thermo Fisher Scientific, USA) was used as the microbial culture medium and prepared according to the manufacturer's instructions. Tryptone soya agar (TSA) was prepared by supplementing TSB with 1.5% w/v Oxoid agar bacteriological (Thermo Fisher Scientific, USA). All media and reagents used for microbial culture were sterilized by autoclaving at 121°C for 30 min before use.

T-2 toxin (> 95% purity) was purchased from Bioaustralis Fine Chemicals, Australia. High-purity, HPLC-grade methanol (MeOH; Honeywell, USA), trifluoracetic acid (TFA; Sigma-Aldrich, USA), and formic acid (FA, Sigma-Aldrich, USA), were used for high-performance liquid chromatography (HPLC) and mass spectrometry (MS) experiments. Water was purified using a Sartorius Stedim Arium Pro VF purification system. Dimethyl sulfoxide (DMSO) utilized in bioassays was of molecular biology grade (Sigma-Aldrich, USA).

Microbial strains

Ten *Bacillus* sp. isolates (BC1 – 10) were used in this study. Seven isolates (BC1 – 7) originated from soil and vegetation and were provided by our collaborator, while the remaining three (BC8 – 10) were isolated from marine samples, as reported in a previous study (Lu et al. 2026). The strains were conserved in 25% glycerol in TSB and stored at – 80°C until further use. For experiments, the strains were revived from the glycerol stocks, maintained on TSA plates and incubated statically at 37°C for 16–20 h. For liquid culture, single colonies were selected from TSA plates and inoculated into TSB, followed by incubation at 37°C for 16–20 h with shaking at 200 rpm.

Taxonomic identification

A single colony of microbial isolates was resuspended in PrepMan Ultra Sample Preparation Reagent (Thermo Fisher Scientific, USA) and submitted to the Australian Genome Research Facility (AGRF; Victoria, Australia) for 16S rRNA gene sequencing, where the 16S rRNA gene was PCR-amplified and Sanger sequenced.

Alternatively, genomic DNA (gDNA) was extracted from bacterial cell pellets obtained from cultures initiated from single colonies using the Monarch High Molecular Weight DNA Extraction Kit (New England Biolabs, USA) following the manufacturer's protocol for Gram-positive bacteria. DNA concentration and purity were measured using a NanoDrop spectrophotometer (Thermo Fisher Scientific, USA). The extracted gDNA was subsequently submitted to Plasmidsaurus (Kentucky, USA) for 16S rRNA gene amplification or to AGRF for PacBio long-read sequencing.

The resulting sequences were compared against the combined 16S databases from the National Center for Biotechnology Information (NCBI) using Basic Local Alignment Search Tool for nucleotides (BLASTn, version 2.17.0) to determine the closest taxonomic assignment (Zhang et al. 2000).

Bacterial growth curve measurements

Bacterial growth curve experiments were carried out based on a previous study using microtiter plates (Krishnamurthi et al. 2021). Specifically, single colonies of bacterial samples from TSA plates were inoculated into separate sterile Eppendorf tubes containing 1 mL of TSB medium and incubated at 37°C for 8 h. Optical density at 600 nm (OD_{600}) of each culture was measured on a DU-730 UV/Vis spectrophotometer (Beckman Coulter, USA), and the cultures were diluted with TSB to a final OD_{600} of approximately 0.001. Subsequently, 196 µL of each diluted culture was mixed with 4 µL of T-2 stock solutions of 4, 2, and 1 mM in DMSO to achieve final toxin concentrations of 80, 40, and 20 µM, respectively. Cultures containing only 2% DMSO were used as controls. The cultures were then transferred into wells of a sterile, clear, flat-bottom 96-well plate (Corning, USA) in duplicate (100 µL per well); TSB (100 µL) was included as blank samples.

The plate was then analyzed using a SpectraMax iD5 multi-mode microplate reader (Molecular Devices, USA), where OD_{600} was automatically acquired every 30 min for 24 h. The temperature in the reading chamber was maintained at 37°C, and the plate was subjected to periodic double-orbital shaking for 5 min before each measurement. Growth curves were generated by plotting the recorded OD_{600} values against respective incubation time. Curve smoothing was performed in Prism (v11.0.0, GraphPad Software, USA), using a moving average method with four neighbouring points on each side.

Bacterial doubling time and specific growth rate were calculated based on a reported protocol (Hall et al. 2014), using the following equation:

$$Doubling\ time = \frac{\ln(2)}{\mu} \times 60\ (min)$$

where μ is the bacterial specific growth rate (h^{-1}), defined as the slope of the linear regression of $\ln(OD_{600})$ versus time (h) during the exponential phases of the bacterial growth curves.

Screening of T-2-metabolizing Bacillus strains

Preparation of toxin-spiked cultures

Screening of *Bacillus* strains capable of degrading T-2 was conducted according to a previous reported method with slight modifications (Hassan et al. 2021). Briefly, diluted bacterial cultures with OD_{600} of approximately 0.001 were prepared as described above. Subsequently, 245 µL of each diluted bacterial culture was mixed with 5 µL of 2 mM T-2 stock solution in DMSO. TSB medium containing only T-2 at the same concentration without bacteria were included as controls. The cultures were incubated at 37°C and collected for analysis at the indicated incubation time points. The final concentrations of T-2 and DMSO in each culture were 40 µM and 2% (v/v), respectively.

HPLC/MS analysis

Following incubation, the toxin-spiked bacterial cultures and controls were collected and mixed with an equal amount of TSB. The samples were then centrifuged at 5,000 rcf for 10 min to collect the supernatant. The supernatant was then sterile filtered through a 0.2 µm syringe filter, and the filtrates were analyzed by HPLC/MS to evaluate the toxin removal. HPLC was performed on a Dionex Ultimate 3000 RS UHPLC system (Thermo Fisher Scientific, USA) consisting of a pump, an autosampler, a diode array detector, and an automatic fraction collector. The column used was an Accucore C18 HPLC column (2.6 µm, 150 × 2.1 mm i.d.; Thermo Fisher Scientific, USA) coupled to a C18 guard column. Chromatographic separation was carried out using a linear gradient of MeOH:H_2O (0.1% FA) from 50:50 to 100:0 (v/v) over 9 min, followed by a 100% MeOH wash for 2 min and a 2-min re-equilibration to the initial 50:50 condition. The injection volume was 20 µL, and the flow rate was 0.25 or 0.3 mL/min. MS analyses were performed on an MSQ Plus single-quadrupole electrospray ionization (ESI) mass spectrometer (Thermo Fisher Scientific, USA) utilizing the total ion chromatogram (TIC) channel.

Remaining toxin was calculated using the following equation:

$$\text{Remaining toxin}\ (\%) = \frac{\mathrm{I_s} - \mathrm{I_{blank}}}{\mathrm{I_c} - \mathrm{I_{blank}}} \times 100$$

where I_s and I_c are the intensities of the toxin peak in the TIC chromatograms of the toxin-spiked bacterial culture and the toxin control without bacterial cells, respectively. I_{blank} is the intensity of the

peak detected at the same retention time as the toxin in the blank solution containing only growth medium.

Isolation and characterization of metabolized products of T-2

Large-scale culture of T-2-degrading Bacillus strain

To accumulate the metabolized product of T-2, a large-scale culture of the active bacterial strain with the toxin was conducted. Specifically, 200 mL of TSB medium containing the bacterial culture at a final OD_{600} of approximately 0.001 was prepared in a 1,000 mL conical flask. The culture was then supplemented with 4.0 mg of T-2 dissolved in 4 mL of DMSO. The flask was incubated at 37°C for 56 h with orbital shaking at 200 rpm. An identical bacterial culture with the absence of T-2 was also prepared as a negative control.

Purification of degradation products of T-2

After incubation, the large-scale culture was centrifuged at 8,000 rpm for 40 min at 4°C to separate the supernatant. The collected supernatant was then partially purified using C18 silica gel solid-phase extraction. Briefly, the supernatant was loaded into a glass column (25 x 4 cm i.d.) prepacked with 60 g of C18 silica gel and allowed to pass completely through the column. The column was then washed with 300 mL of water to remove highly polar components, followed by elution with 300 mL of MeOH. The MeOH eluate was collected and dried under vacuum to obtain the MeOH fraction (180 mg).

The MeOH fraction was further fractionated by reverse-phase HPLC, utilizing a Betasil C18 column (150 x 21.2 mm i.d., 5 µm; Thermo Fisher Scientific, USA). Chromatographic separation was achieved using a linear MeOH:H_2O (0.1% TFA) gradient from 25:75 to 85:15 (v/v) over 50 min, followed by a 10-min wash with 100% MeOH, at a flow rate of 9 mL/min. Fractions were collected automatically at 1-min intervals, yielding a total of 60 subfractions. The collected fractions were analyzed by HPLC/MS under the previously described conditions, and the purified metabolite of T-2 was detected at subfraction 41 (4.3 mg).

Structural characterization of T-2 degradation product

NMR spectroscopy was used to elucidate the chemical structures of the isolated compounds and was recorded on an Ascend 800 MHz spectrometer coupled to a TCI CryoProbe (Bruker, USA) at 298 K in DMSO-d_6 (Cambridge Isotope Laboratories Inc., USA). Chemical shifts were referenced to the residual solvent peaks of DMSO-d_6 (δ_H 2.50 and δ_C 39.52). All NMR data were processed with MestReNova software (v14.3.3, Mestrelab Research, Spain).

Toxicity assessment

Cell culture

Human embryonic kidney-derived cells (HEK293T; CRL-3216, American Type Culture Collection, USA) were maintained in growth medium comprising high-glucose Dulbecco's modified Eagle's medium (DMEM, Sigma-Aldrich, USA) with 10% fetal bovine serum (FBS, Thermo Fisher Scientific, USA) in a humidified incubator containing 5% CO_2 at 37°C. The cells were sub-cultured when reaching approximately 80% confluence with standard trypsinization processes.

Cytotoxicity assay

The toxicity of T-2 and its degraded product was evaluated on HEK293T cells using a standard MTT (3-(4,5-dimethylthiazol-2-yl)-2,5-diphenyltetrazolium bromide) assay (van Meerloo et al. 2011). HEK293T cells were initially seeded into tissue culture-treated 96-well plates (Corning, USA) at a density of 10,000 cells per well in 100 µL of growth medium in triplicate and incubated for 24 h. The medium was then replaced with fresh medium containing the test compounds at final concentrations of 0, 1.95, 3.9, 7.8, 15.6, 31.2, 62.5, and 125 nM, followed by a further incubation for 24 h. After incubation, the treatments were removed and replaced with 100 µL of MTT (Sigma-Aldrich, USA) solution (0.5 mg/mL in growth medium), and the plates were further incubated for 2 h at 37°C. The MTT solution was then aspirated, and 150 µL DMSO was added to each well to dissolve the formazan crystals by shaking on an orbital shaker for 15 min. Absorbance at 550 nm was measured using a SpectraMax iD5 multi-mode microplate reader (Molecular Devices, USA). During treatment, the final DMSO concentration in each well was maintained at 0.5% (v/v). DMSO (0.5%, v/v) served as a vehicle control. Cell viability was expressed as a percentage of the vehicle control, using absorbance values from the MTT assay.

Statistical analysis

Experiments were conducted in duplicates or triplicates, and data were expressed as means ± standard deviation (SD). Curve fitting and half-maximal effective concentration (EC_{50}) calculation were performed in Prism software (v11.0.0, GraphPad Software, USA). Statistical significance was evaluated using *t*-tests on log-transformed raw data, where $p < 0.05$ was considered statistically significant.

Results

Taxonomic identification

Taxonomic identification of the ten microbial strains investigated in this study (BC1 – 10) was performed by 16S rRNA gene sequencing using genomic DNA extracted from pure microbial isolates. The bacterial nucleotide sequences were compared against the NCBI 16S ribosomal RNA sequence database for bacteria and archaea using basic local alignment search tool for nucleotides (BLASTn) method to identify closely related strains. The closest matches with the highest identity scores for BC1 – 10 are summarized in Table 1.

Table 1
Taxonomic details by 16S rRNA sequence BLASTn search for BC1–10.

Strain	Closest taxonomic match	Hit length (base pair, bp)	Identity (%)	Accession number
BC1	*B. subtilis*	1454	98.71	NR_113265.1
BC2	*B. paranthracis*	1477	98.86	NR_157728.1
BC3	*B. subtilis*	1457	98.58	NR_113265.1
BC4	*B. subtilis*	756	99.87	FJ263034.1
BC5	*B. subtilis*	1469	99.73	NR_112629.1
BC6	*B. subtilis*	1446	98.10	NR_113265.1
BC7	*B. subtilis*	1467	99.59	NR_113265.1
BC8	*B. megaterium*	725	100	FJ685762.1
BC9	*Bacillus* sp. WJ08	719	100	HM045832.1
BC10	*B. subtilis* subsp. *subtilis* 168	718	100	ABQK01000001.1

As shown in Table 1, all ten microbial strains were closely related to the genus *Bacillus*, with most strains showing high sequence similarity to bacteria in the *Bacillus subtilis* group, including *B. rugosus*, *B. megaterium*, and multiple different *B. subtilis* strains. One strain, BC2, was highly comparable to *B. paranthracis*, a member of the *Bacillus cereus* group, with an identity of 98.86%. Query coverage for the BLASTn search was 100% for most strains, and sequence identity values were greater than 98%, supporting their taxonomic assignment as *Bacillus* spp.

Bacterial growth curve analysis

Prior to conducting degradation assays, growth curves of the ten *Bacillus* strains under the presence of multiple T-2 concentrations were generated to evaluate whether the toxin affected bacterial proliferation and growth under the experimental conditions (Fig. 1). The bacteria were inoculated into TSB medium supplemented with T-2 at final concentrations of 80, 40, 20, or 0 μM (control), respectively, and incubated at 37°C; OD_{600} was then measured at 30-min intervals over 24 h. Growth curves for each culture were constructed by plotting their OD_{600} values against the corresponding incubation times, as presented in Fig. 1.

Generally, for each bacterial strain, growth curves at different T-2 concentrations (blue, red, and green curves) possessed patterns comparable to those of the untreated controls (black curves), with minimal differences in OD_{600} intensities. This suggested T-2 had limited impact on the growth performance of the tested *Bacillus* strains.

Most strains exhibited biphasic, diauxic-like growth features, with an initial lag phase during the first 3 h and a primary exponential phase occurring approximately between 3 and 8 h. Most cultures reached an initial OD_{600} peak at around 8 h, followed by a slight decrease between 8 and 14 h and a secondary rise afterwards. This pattern, however, was not seen in all strains. BC8 and BC9 did not show a clear trough-and-recovery profile and instead exhibited a sustained increase in OD_{600} after the primary growth phase. In contrast, BC4 displayed a continued OD_{600} decrease without recovery after reaching its peak at 8 h. No clear death phase was observed within the 24 h monitoring period for all cultures, suggesting the bacteria were likely viable beyond the experiment timeframe.

To quantitatively compare the proliferation among strains, their specific growth rate and doubling time were calculated and are presented in Table 2. These parameters are commonly used in growth-curve analysis and provide useful information on bacterial growth performance (Hall et al. 2014).

Table 2

Specific growth rates (h^{-1}) and doubling time (min) for BC1–10 in T-2-free TSB medium at 37°C.

Strain	Exponential phase used[a]	Specific growth rate (h^{-1})[b]	Doubling time (min)[b]
BC1	4–6.5 h	1.05 ± 0.003	39.52 ± 0.13
BC2	3–4.5 h	1.30 ± 0.05	32.02 ± 1.18
BC3	4–6.5 h	1.22 ± 0.03	34.20 ± 0.95
BC4	3.5–5.5 h	0.80 ± 0.01	52.17 ± 0.73
BC5	3.5–6.5 h	1.08 ± 0.01	38.58 ± 0.47
BC6	4–6.5 h	1.00 ± 0.03	41.79 ± 1.07
BC7	3–6.5 h	1.09 ± 0.01	38.32 ± 0.50
BC8	4–6.5 h	1.16 ± 0.01	35.76 ± 0.43
BC9	3.5–6.5 h	0.84 ± 0.01	49.63 ± 0.70
BC10	3.5–5.5 h	1.12 ± 0.04	37.06 ± 1.27

[a] The time frame during exponential phase where $\ln(OD_{600})$ increased linearly overtime.

[b] Data expressed as mean ± standard deviation (n = 2)

As seen in Table 2, most *Bacillus* strains displayed comparable specific growth rates under the tested conditions. BC2 showed the highest growth rate of 1.30 ± 0.05 h^{-1}, while BC9 and BC4 proliferated at lower rates of 0.84 ± 0.01 and 0.80 ± 0.05 h^{-1}, respectively. Consistently, BC2 had the shortest doubling time (32.02 ± 1.18 min), and the longest doubling time was corresponding to BC4 (52.17 ± 0.73 min). Overall, the strains exhibited rapid growth in T-2-free medium, with doubling times ranging from

approximately 30 to 60 min, broadly consistent with reported doubling times for *Bacillus* species (Beranová et al. 2010; Hageman et al. 1984).

Due to the high similarity between the growth curves of T-2-treated and control cultures, the growth rates and doubling time for cultures with T-2 were generally comparable to those of the corresponding untreated controls. However, BC1 treated with 80 μM T-2 had a slightly slower growth rate (0.88 h^{-1}) than the untreated BC1 culture (1.05 h^{-1}), possibly due to a small decrease in OD_{600} during the exponential phase for this culture (Fig. 1). This suggested this strain was slightly sensitive to T-2 at high concentration.

Based on these observations, T-2 at 40 μM was selected for the subsequent degradation assay, as cultures exposed to this concentration showed minimal growth differences from the toxin-free controls.

Screening of T-2-removing Bacillus strains

Chemically, T-2 is a sesquiterpene with a tetracyclic 12,13-epoxytrichothec-9-ene core skeleton (Fig. 2A) (Samara et al. 1987). Due to the lack of strong chromophores and fluorophores in the structure, T-2 possesses relatively weak UV/Vis absorption and fluorescence, making its detection with UV/Vis and fluorescence detectors unreliable and potentially misleading (Meneely et al. 2023). As a result, mass spectrometry (MS) utilizing total ion chromatogram (TIC), which directly visualize ions detected instead of relying on optical absorption, was primarily used to monitor the presence of T-2 in this study. Screening of *Bacillus* strains capable of removing T-2 was performed *in vitro* where the bacteria were inoculated into growth media containing 40 μM T-2. After a 48-hour incubation, the cultures were centrifuged, and the filtered supernatants were analyzed with HPLC/MS to detect and quantify the remaining amount of T-2 in the cultures. The results are summarized in Fig. 2B.

Among the ten *Bacillus* cultures tested, BC2, BC6, and BC9 significantly reduced T-2 levels after 48 h of incubation (Fig. 2B). BC2 exhibited the strongest T-2 decontamination activity, achieving nearly complete toxin removal within 48 h ($p < 0.0001$). BC6 and BC9 also showed notable activity, reducing T-2 level by approximately 50% over the same incubation period ($p < 0.001$). In contrast, the remaining strains showed limited or no effect on T-2 reduction, with toxin levels in these cultures remaining comparable to that observed in the control after incubation.

To study the T-2 removal rate of BC2, BC6, and BC9, kinetic assays were performed by monitoring T-2 levels at multiple incubation time points (Fig. 2C). For BC2, T-2 levels were assessed after 8, 16, 24, 32, and 48 h of incubation, while BC6 and BC9 were evaluated every 24 h over a 4-day period. As shown in Fig. 2C, all three cultures reduced T-2 levels in a time-dependent pattern. For example, BC2 culture exerted minimal T-2 reduction of around 10% during the first 16 h. However, the toxin level decreased significantly by approximately 70% at 24 h and further declined to nearly 0% by 48 h. In contrast, BC6 and BC9 showed slower T-2 removal rates, with both cultures achieving comparable toxin reduction of approximately 50% during the first 48 h. After 48 h, the reduction rate for BC6 further slowed down, leaving approximately 35% of T-2 remaining at 96 h, while BC9 exhibited a better profile, with only around

5% T-2 left at 96 h. Overall, BC2 exhibited the most rapid T-2 removal, while BC9 achieved greater T-2 reduction than BC6 over the extended incubation period.

LC/MS identification of T-2 metabolized product

Given BC2, BC6, and BC9 exhibited T-2 removal activity, the cultures were further investigated by HPLC/MS to determine whether the toxin was metabolized into detectable transformation products. This was done by analyzing the HPLC/TIC spectra of the cultures over time. Figure 3 presents the full stacked HPLC/TIC spectra obtained at different incubation time for the three active cultures. For BC2 (Fig. 3A), T-2 was detected at a retention time of approximately 7.0 min; this was supported by the ESI-MS analysis of the corresponding peak, which gave adduct ions at *m/z* 489 $[M + Na]^+$ and 955 $[2M + Na]^+$ (Fig. 3D, top), consistent with the molecular weight of T-2. As incubation time increased, the intensity of this peak progressively decreased, reaching a nearly undetectable amount at 32 h. Concurrently, a distinct peak at around 5.5 min rose in intensity over time from 8 h. Compared with other peaks across the spectra, the 5.5-min peak was the main chromatographic feature that showed an inverse relationship with the T-2 peak in a time-dependent manner, suggesting this peak represented the main metabolism product of T-2 by BC2. ESI-MS analysis of this peak showed an ion at *m/z* 447 (Fig. 3D, bottom), indicating part of the T-2 structure was cleaved during bacterial metabolism.

Similar patterns were noted in the stacked TICs of BC6 (Fig. 3B) and BC9 (Fig. 3C), where the time-dependent formation of the major T-2 degradation product at around 6.8 min was accompanied by a reciprocal decrease of the T-2 peak at approximately 8.1 min. A slight shift in retention time was observed for peaks detected in BC6 and BC9 cultures compared to those in BC2; this was due to the different chromatographic flow rates used for these analyses, as indicated in the Fig. 3 caption. Despite these retention-time differences, MS analysis showed that the transformation product detected in all three cultures had the same ion at *m/z* 447, suggesting BC2, BC6, and BC9 produced the same major T-2 transformation product. In summary, HPLC/MS analysis indicated that the three active cultures converted T-2 into a common major detectable metabolite.

Isolation and structural characterization of the biodegraded product of T-2

Since a potential T-2 biotransformation product was detected by HPLC/MS, a larger-scale culture experiment was performed to accumulate sufficient amount for purification and characterization of this compound. BC2 was selected for this experiment as it showed the most efficient T-2 metabolism activity among the three active strains (Fig. 2C). Briefly, BC2 was inoculated into 200 mL of TSB medium supplemented with 4 mg of T-2 and incubated at 37°C with shaking. The culture was periodically analyzed by HPLC/MS to monitor the toxin transformation overtime, and the stacked TIC chromatograms obtained at various incubation time are shown in Fig. 4A.

Compared to the small-scale BC2 experiment (Fig. 3A), the larger-scale culture exhibited slower T-2 transformation, requiring up to 56 h rather than 32 h to eliminate T-2 (Fig. 4A). As anticipated, the product

peak with an ion at *m/z* 447, detected as retention time around 6 min, was present in the culture. Interestingly, from 44 h onward, an additional peak at retention time of approximately 8.2 min began to appear and increased in intensity overtime. This peak was not observed in the small-scale degradation assay for BC2 and gave an ion at *m/z* 403 in the positive-mode ESI-MS analysis. Based on these observations, the *m/z* 447 and 403 peaks were selected for purification and were labelled as compounds **1** and **2**, respectively (Fig. 4A).

To isolate compounds **1** and **2**, the large-scale culture at 56h was collected and centrifuged to give the supernatant, which was then partially purified by C18 solid-phase extraction using H_2O and MeOH sequentially. The water partition, containing highly polar constituents, was discarded, while the MeOH fraction was collected for subsequent purification by reverse-phase HPLC which gave a total of 60 subfractions (**Fig. S1**, **Supporting Information**). Due to the low UV profiles of the compounds, the subfractions were monitored individually with MS, and compounds **1** and **2** were obtained at subfractions 41 and 50, respectively.

The isolated compounds were structurally elucidated using NMR spectroscopy. The ^{1}H NMR data of **1** (Table 3) displayed several characteristic proton resonances of the 12,13-epoxytrichothec-9-ene backbone (Fig. 2A), such as the C13 methylene proton pair at δ_H 2.87 and 2.66, the olefinic proton of C10 at δ_H 5.65, as well as the C14 and C16 methyl singlets at δ_H 0.63 and 1.65, respectively (Savard et al. 1987). Comparison of the ^{1}H and ^{13}C NMR data of **1** with those of T-2 (Table 3) revealed a high degree of structural similarity between the two compounds. The most obvious difference was the absence of resonances corresponding to an acetyl moiety in compound **1**, including a quaternary carbonyl carbon and an α-methyl proton signals, suggesting **1** was a deacetylated product of T-2. Furthermore, there was a notable upfield shift of proton H4 in compound **1** (δ_H 4.08) compared to that in T-2 (δ_H 5.47) (Table 3), indicating the deacetylation occurred at position C4. The other NMR data (**Fig. S3**-**7**, **Supporting Information**) also supported this structural assignment; and the ion observed at *m/z* 447 was the sodium adduct of **1**, matching the molecular weight of 424 amu for this compound. Based on the findings, compound **1** was identified as 4-deacetylated T-2 toxin, also known as HT-2 toxin (HT-2) (Fig. 4B).

Table 3

Comparison of ^{1}H (800 MHz, DMSO-d_6) and ^{13}C (200 MHz, DMSO-d_6) NMR data for compound **1** and T-2 toxin.

Position	Compound 1		T-2 toxin	
	δ_H, mult. (*J* in Hz)	**δ_C, type**	**δ_H, mult. (*J* in Hz)**	**δ_C, type**
1	–	–	–	–
2	3.27, d (4.8)	78.6, CH	3.42, d (4.8)	78.4, CH
3	3.87, dd (3.2, 4.8)	78.9, CH	4.07, m	75.9, CH
4	4.08, d (3.2)	79.6, CH	5.47, d (3.2)	82.2, CH
5	–	48.1, C	–	48.3, C
6	–	42.0, C	–	42.4, C
7	2.22, dd (5.6, 15.2), H_α 1.88, d (15.2), H_β	26.6, CH_2	2.24, dd (5.6, 15.2), H_α 1.86, d (15.2), H_β	26.7, CH_2
8	5.19, d (5.6)	67.8, CH	5.22, d (5.6)	67.5, CH
9	–	134.6, C	–	134.9, C
10	5.65, d (5.6)	124.6, CH	5.70, d (5.6)	124.1, CH
11	4.01, d (5.6)	66.3, CH	4.18, d (5.6)	66.3, CH
12	–	64.5, C	–	64.3, C
13	2.87, d (4.0), H_α 2.66, d (4.0), H_β	45.5, CH_2	2.99, d (4.0), H_α 2.81, d (4.0), H_β	46.3, CH_2
14	0.63, s	7.0, CH_3	0.59, s	6.4, CH_3
15	4.06, d (12.0), H_α 3.83, d (12.0), H_β	64.1, CH_2	4.17, d (12.8), H_α 3.95, d (12.8), H_β	64.0, CH_2
16	1.65, s	19.9, CH_3	1.66, s	19.8, CH_3
17	–	171.7, C	–	171.7, C
18	2.08, m	42.8, CH_2	2.09, m	42.8, CH_2
19	1.96, m	25.2, CH	1.96, m	25.2, CH
20	0.90, d (6.4)	22.1, CH_3	0.89, d (6.4)	22.1, CH_3

Position	Compound 1		T-2 toxin	
	δ_H, mult. (*J* in Hz)	δ_C, type	δ_H, mult. (*J* in Hz)	δ_C, type
21	0.89, d (6.4)	22.2, CH_3	0.89, d (6.4)	22.2, CH_3
4-OAc	–	–	2.04, s, CH_3	20.7, CH_3
				170.3, CO
15-OAc	1.97, s, CH_3	20.8, CH_3	1.97, s, CH_3	20.8, CH_3
		169.8, CO		169.7, CO

Compound **2** was elucidated as a tetradepsipeptide, consisting of four units of amino acids and their analogues, D-*O*-Leu-D-Ala-L-*O*-Val-L-Val (Fig. 4B). Its NMR data were provided in the **Supporting Information** (**Fig. S8-12**). However, this compound is regarded as a bacterial secondary metabolite secreted by members of *B. cereus* group and therefore not considered as part of the T-2 metabolism (Marxen et al. 2015; Naka et al. 2020).

In vitro toxicity assessment of T-2 and HT-2 on HEK293T cells

As T-2 is toxic to several organs including the kidneys, the toxicity of T-2 and its biodegradation product HT-2 was examined on a human embryonic kidney-derived cell line (HEK293T), which is a standard *in vitro* mammalian model for assessing the general cytotoxic effects of small molecules. Cells were exposed to various concentrations of the samples (0–125 nM), and cell viability was assessed by MTT assay (Fig. 5).

As shown in Fig. 5, HEK293T cells were sensitive to both T-2 and HT-2 at nanomolar concentrations; however, cell viability reached a plateau of approximately 50% at concentrations above 3.9 nM for T-2 and 31.2 nM for HT-2, with no further decrease observed at higher concentrations. This pattern may indicate the compounds exerted a predominantly growth-inhibitory effect under the tested conditions. Apparently, T-2 showed stronger inhibitory activity than HT-2 in HEK293T cells. For example, exposure to 3.9 nM T-2 reduced cell viability by around 50%, while HT-2 at the same concentration had minimal effect, maintaining cell viability close to 100% (Fig. 5). Both treatments reduced cell viability in a dose-dependent manner, with calculated apparent half-maximal effective concentrations (EC_{50}) of 1.77 and 12.76 nM for T-2 and HT-2, respectively. These results suggested that HT-2 was less toxic than T-2 in HEK293T cells.

Discussion

Biological degradation of mycotoxins is a promising approach to mitigate their contamination, offering several advantages over traditional removal strategies. Various microbial strains have been reported to decontaminate mycotoxins, among which *Bacillus* species have gained attention as promising

candidates due to their emerging toxin biotransformation ability. In this study, we aim to further elucidate the role of *Bacillus* bacteria in degrading T-2 by assessing their toxin removal capacity, characterizing the toxin biotransformation products, as well as evaluating the toxicity of these products.

Ten microbial strains used in this study (BC1 – 10) were taxonomically assigned as *Bacillus* spp., supported by 16S rRNA gene sequencing (Table 1), with most strains showing high similarity to members of the *B. subtilis* family, except for BC2 which was closely related to *B. cereus* group. Comparison of growth curves between T-2-free and T-2-treated cultures (Fig. 1) revealed that the tested bacterial strains exhibited relatively high tolerance to T-2. In most cases, the growth rates and doubling time in T-2-spiked medium were comparable with those observed in T-2-free cultures, suggesting T-2 had limited inhibitory effects on the proliferation of these *Bacillus* strains.

Bacteria are generally believed to have higher resistance to trichothecene mycotoxins than mammalian cells (Haschek 1989). This may be partly due to trichothecenes, particularly T-2, having high-affinity bindings to eukaryotic ribosomes, which are structurally different to bacterial ribosomes, resulting in inhibition of protein synthesis primarily in eukaryotic cells (Middlebrook and Leatherman 1989; Rocha et al. 2005). Consistent findings have also been reported in previous studies where several bacteria, including *Bacillus* spp., were generally not affected by this type of mycotoxins (Madhyastha et al. 1994).

BC1–10 were evaluated for their T-2 removal activity, with strains BC2, BC6, and BC9 demonstrating substantial *in vitro* T-2 decontamination, indicating that this capability was strain-dependent rather than a general feature for *Bacillus* bacteria. Furthermore, the activity was time-dependent, where longer incubation time led to lower residual T-2 for all three strains (Fig. 2). BC2 stood out from others as having the most rapid removal rate, achieving near-complete T-2 elimination within 48 h. This may be partly related to the relatively rapid growth rate of this strain compared to others (Table 2).

HPLC/MS and NMR analysis confirmed the toxin removal was associated with metabolism of T-2, with the active strains transforming the toxin to HT-2 through deacetylation at C4. In animals and other biological systems, T-2 is known to frequently undergo hydrolysis, deacetylation, hydroxylation, and glucuronidation during metabolism, and conversion of T-2 to HT-2 is a well-recognized metabolic route (Ohta et al. 1977; Righetti et al. 2019; Sun et al. 2015). For instance, HT-2 was identified as a major metabolite of T-2 in broiler chicken plasma (Sun et al. 2015); Yang and coauthors demonstrated that T-2 was metabolized to various products including HT-2 in liver microsomes of several farm animals (Yang et al. 2017); while Righetti and colleagues observed this transformation in wheat (Righetti et al. 2019). In microorganisms, this conversion has been confirmed in bacteria such as in *Curtobacterium* and *Eubacterium* species, as well as in several soil and water bacterial communities (Beeton and Bull 1989; Fuchs et al. 2002; Ueno et al. 1983). Decontamination of T-2 has been observed in several *Bacillus* strains; however, most studies have mainly focused on general toxin reduction, and metabolism of this toxin to other products is poorly documented for this genus (García-García et al. 2024; Hassan et al. 2021). Ma and coauthors discovered a *Bacillus* sp. from wheat that converted T-2 to neosolaniol instead of HT-2 (Ma et al. 2023). Therefore, the identification of HT-2 as the major transformation product in the

present *Bacillus* cultures provides additional evidence that T-2 deacetylation can occur in *Bacillus* bacteria.

Although this current study did not specifically identify the mechanisms underlying this conversion in the tested *Bacillus* species, the cleavage of the ester group at C4 strongly suggested the involvement of hydrolytic activity, which may be mediated by enzymes such as esterases or carboxyesterases capable of targeting ester bonds in T-2. This pathway is biologically plausible because *Bacillus* bacteria are well-recognized for their ability to produce a wide range of intra- and extra- cellular enzymes including laccases, esterases, carboxypeptidases, and peroxidases, some of which have been implicated in the degradation of other mycotoxins such as aflatoxins, zearalenone, and ochratoxins (Nguyen et al. 2024; Qin et al. 2021; Qing et al. 2021; Sun et al. 2023).

The ultimate goal of mycotoxin biodegradation is detoxification, whereby the resulting biotransformation products exhibit substantially reduced toxicity or, ideally, are non-toxic (Nguyen et al. 2024; Vanhoutte et al. 2016). In animal industry, mycotoxin detoxification not only protects livestock health but also reduces potential mycotoxin-related risks associated with animal-derived food products, such as eggs, meat, and milk. For type A trichothecenes like T-2, effective detoxification is generally associated with removal of the C12-C13 epoxide ring, as well as substitution of key functional groups such as the C3 hydroxyl and the C9-C10 double bond (Qinghua et al. 2013). Structural modification at C4 has also showed reduction in toxicity (Wang et al. 2021). Indeed, the cytotoxicity assay on HEK293T in this current study indicated that HT-2 was less toxic than T-2, as reflected by a nearly 7-fold higher EC_{50} value (Fig. 5), supporting the view that bacterial transformation reduced the relative toxicity of the parent toxin. However, HT-2 remained active within the nanomolar concentration range and is still recognized as a toxic trichothecene, often considered together with T-2 in safety assessments (Meneely et al. 2023). Constituently, from a safety perspective, conversion of T-2 to HT-2 represents a meaningful but incomplete detoxification process.

Overall, this study provides evidence that the selected *Bacillus* strains can effectively reduce T-2 toxin levels through biotransformation *in vitro*. Several *Bacillus* species, especially members of the *B. subtilis* group, have been extensively studied for beneficial applications, including their use as probiotics and feed additives to support general health (Payne et al. 2024). The present findings provide further insight into the understanding of T-2 mycotoxin metabolism by these bacteria and signify their potential usage as microbial additives to mitigate mycotoxin contamination. Notwithstanding, given the partial detoxification of T-2, further safety research is required to ensure a secure and meaningful translation of these strains in food and feed industry.

Abbreviations

T-2	T-2 toxin
HT-2	HT-2 toxin

HPLC/MS	High-performance Liquid Chromatography/Mass Spectrometry
NMR	Nuclear Magnetic Resonance

Declarations

Acknowledgments

This research was supported by the Commonwealth through an Australian Government Research Training Program Scholarship [DOI: https://doi.org/10.82133/C42F-K220].

Thanh D. Nguyen thanks Griffith University, Australia for the Griffith University Postgraduate Research Scholarship (GUPRS) [https://www.griffith.edu.au/research-study/scholarships/guprs]. The authors also acknowledge Bioproton Pty Ltd, Queensland, Australia, for providing the microbial strains used in this study and for additional supports toward laboratory consumables.

Conflicts of Interest

Xiaojing Chen was employed by Bioproton Pty Ltd, Queensland, Australia. The authors declare no other conflicts of interest.

CRediT Authorship Contribution Statement

Thanh Duy Nguyen: Conceptualization, data curation, formal analysis, investigation, validation, visualization, writing – original draft, writing – review and editing. **Yaoying Lu**: Investigation, data curation, writing – review and editing. **Xiaojing Chen**: Conceptualization, writing – review and editing, resources, supervision, project administration. **Linlin Ma**: Validation, writing – review and editing, supervision. **Yunjiang Feng**: Conceptualization, writing – review and editing, supervision, project administration.

Declaration of Generative AI and AI-assisted Technologies in the Manuscript Preparation Process

During the preparation of this work, the author(s) used generative artificial intelligence (AI) technologies, ChatGPT (GPT-5.5, OpenAI, https://www.chatgpt.com) in order to support drafting and polishing the academic language of the manuscript. After using this tool/service, the author(s) reviewed and edited the content as needed and take(s) full responsibility for the content of the published article.

Data Availability Statement

Data supporting the findings are provided within the manuscript and the Supplementary Information files.

References

1. Adebo, O. A. et al. A review on novel non-thermal food processing techniques for mycotoxin reduction. *Int. J. Food Sci. Technol.* **56**, 13–27. https://doi.org/10.1111/ijfs.14734 (2021).
2. Beeton, S. & Bull, A. T. Biotransformation and detoxification of T-2 toxin by soil and freshwater bacteria. *Appl. Environ. Microbiol.* **55**, 190–197. https://doi.org/10.1128/aem.55.1.190-197.1989 (1989).
3. Beranová, J., Mansilla, M. C., Mendoza Dd, Elhottová, D. & Konopásek, I. Differences in Cold Adaptation of *Bacillus subtilis* under Anaerobic and Aerobic Conditions. *J. Bacteriol.* **192**, 4164–4171. https://doi.org/10.1128/jb.00384-10 (2010).
4. Chen, C. et al. Enhancing Lignocellulose Degradation and Mycotoxin Reduction in Co-Composting with Bacterial Inoculation. 13:677. (2025). https://doi.org/10.3390/microorganisms13030677
5. Chen, P. et al. Recent advances on type A trichothecenes in food and feed: Analysis, prevalence, toxicity, and decontamination techniques. *Food Control*. **118**, 107371. https://doi.org/10.1016/j.foodcont.2020.107371 (2020).
6. Cundliffe, E., Cannon, M. & Davies, J. Mechanism of Inhibition of Eukaryotic Protein Synthesis by Trichothecene Fungal Toxins. *Proc. Natl. Acad. Sci. U S A*. **71**, 30–34. https://doi.org/10.1073/pnas.71.1.30 (1974).
7. Fuchs, E., Binder, E. M., Heidler, D. & Krska, R. Structural characterization of metabolites after the microbial degradation of type A trichothecenes by the bacterial strain BBSH 797. *Food Addit. Contam.* **19**, 379–386. https://doi.org/10.1080/02652030110091154 (2002).
8. Garai, E. et al. Qualifying the T-2 Toxin-Degrading Properties of Seven Microbes with Zebrafish Embryo Microinjection Method. *Toxins (Basel)*. **12**, 460. https://doi.org/10.3390/toxins12070460 (2020).
9. García-García, F. A. et al. Study of *Bacillus cereus* as an Effective Multi-Type A Trichothecene Inactivator. *Microorganisms* **12**, 2236. https://doi.org/10.3390/microorganisms12112236 (2024).
10. Greco, D. et al. Unlocking the Potential of *Bacillus subtilis*: A Comprehensive Study on Mycotoxin Decontamination, Mechanistic Insights, and Efficacy Assessment in a Liquid Food Model. Foods, **14**:360. (2025). https://doi.org/10.3390/foods14030360
11. Hageman, J. H. et al. Single, chemically defined sporulation medium for *Bacillus subtilis*: growth, sporulation, and extracellular protease production. *J. Bacteriol.* **160**, 438–441. https://doi.org/10.1128/jb.160.1.438-441.1984 (1984).
12. Hall, B. G., Acar, H., Nandipati, A. & Barlow, M. Growth Rates Made Easy. *Mol. Biol. Evol.* **31**, 232–238. https://doi.org/10.1093/molbev/mst187 (2014).
13. Hamad, G. M. et al. A review of recent innovative strategies for controlling mycotoxins in foods. *Food Control*. **144**, 109350. https://doi.org/10.1016/j.foodcont.2022.109350 (2023).
14. Haschek, W. M. Mutagenicity and Carcinogenicity of T-2 Toxin. In: (ed Beasley, V. R.) Trichothecene Mycotoxicosis Pathophysiologic Effects, 1 edn. CRC, Boca Raton, Florida, 63–72. https://doi.org/10.1201/9781315121284 (1989).

15. Hassan, Z. U., Al Thani, R., Alsafran, M., Migheli, Q. & Jaoua, S. Selection of *Bacillus* spp. with decontamination potential on multiple *Fusarium* mycotoxins. *Food Control*. **127**, 108119. https://doi.org/10.1016/j.foodcont.2021.108119 (2021).
16. Ihara, T. et al. Apoptotic cellular damage in mice after T-2 toxin-induced acute toxicosis. *Nat. Toxins*. **5**, 141–145. https://doi.org/10.1002/19970504NT3 (1997).
17. Janik, E. et al. T-2 Toxin—The Most Toxic Trichothecene Mycotoxin: Metabolism, Toxicity, and Decontamination Strategies. *Molecules* **26**, 6868. https://doi.org/10.3390/molecules26226868 (2021).
18. Ji, C., Fan, Y. & Zhao, L. Review on biological degradation of mycotoxins. *Anim. Nutr.* **2**, 127–133. https://doi.org/10.1016/j.aninu.2016.07.003 (2016).
19. Krishnamurthi, V. R., Niyonshuti, I. I., Chen, J. & Wang, Y. A new analysis method for evaluating bacterial growth with microplate readers. *PLoS One*. **16**, e0245205. https://doi.org/10.1371/journal.pone.0245205 (2021).
20. Lu, Y., Chen, X. & Feng, Y. Development of an Integrated Screening Framework for Marine-Derived *Bacillus* Probiotics. *Mar. Drugs*. **24**, 137. https://doi.org/10.3390/md24040137 (2026).
21. Luo, Y., Liu, X. & Li, J. Updating techniques on controlling mycotoxins - A review. *Food Control*. **89**, 123–132. https://doi.org/10.1016/j.foodcont.2018.01.016 (2018).
22. Ma, Y. et al. Screening, Identification and Action Mechanism of T-2 toxin-degrading Strains. *Sh Kexue*. **44**, 173–182. https://doi.org/10.7506/spkx1002-6630-20221111-126 (2023).
23. Madhyastha, M. S., Marquardt, R. R., Masi, A., Borsa, J. & Frohlich, A. A. Comparison of Toxicity of Different Mycotoxins to Several Species of Bacteria and Yeasts: Use of *Bacillus brevis* in a Disc Diffusion Assay. *J. Food Prot.* **57**, 48–53. https://doi.org/10.4315/0362-028X-57.1.48 (1994).
24. Marxen, S. et al. Depsipeptide Intermediates Interrogate Proposed Biosynthesis of Cereulide, the Emetic Toxin of *Bacillus cereus*. *Sci. Rep.* **5**, 10637. https://doi.org/10.1038/srep10637 (2015).
25. McCormick, S. P., Price, N. P. J. & Kurtzman, C. P. Glucosylation and Other Biotransformations of T-2 Toxin by Yeasts of the *Trichomonascus* Clade. *Appl. Environ. Microbiol.* **78**, 8694–8702. https://doi.org/10.1128/AEM.02391-12 (2012).
26. McCormick, S. P., Stanley, A. M., Stover, N. A. & Alexander, N. J. Trichothecenes: From Simple to Complex Mycotoxins. *Toxins (Basel)*. **3**, 802–814. https://doi.org/10.3390/toxins3070802 (2011).
27. Meneely, J., Greer, B., Kolawole, O. & Elliott, C. T-2 and HT-2 Toxins: Toxicity, Occurrence and Analysis: A Review. *Toxins (Basel)*. **15**, 481. https://doi.org/10.3390/toxins15080481 (2023).
28. Middlebrook, J. L. & Leatherman, D. L. Binding of T-2 toxin to eukaryotic cell ribosomes. *Biochem. Pharmacol.* **38**, 3103–3110. https://doi.org/10.1016/0006-2952(89)90021-X (1989).
29. Naka, T. et al. Chemical structure of hydrolysates of cereulide and their time course profile. *Bioorg. Med. Chem. Lett.* **30**, 127050. https://doi.org/10.1016/j.bmcl.2020.127050 (2020).
30. Nayakwadi, S. et al. Toxicopathological studies on the effects of T-2 mycotoxin and their interaction in juvenile goats. *PLoS One*. **15**, e0229463. https://doi.org/10.1371/journal.pone.0229463 (2020).

31. Nguyen, T., Chen, X., Ma, L. & Feng, Y. Mycotoxin Biodegradation by *Bacillus* Bacteria—A. *Rev. Toxins (Basel)*. **16**, 478. https://doi.org/10.3390/toxins16110478 (2024).
32. Ohta, M., Ishii, K. & Ueno, Y. Metabolism of Trichothecene Mycotoxins: I. Microsomal Deacetylation of T-2 Toxin in Animal Tissues. *J. Biochem.* **82**, 1591–1598. https://doi.org/10.1093/oxfordjournals.jbchem.a131854 (1977).
33. Payne, J., Bellmer, D., Jadeja, R. & Muriana, P. The Potential of *Bacillus* Species as Probiotics in the Food Industry: A Review. *Foods* **13**, 2444. https://doi.org/10.3390/foods13152444 (2024).
34. Qin, X. et al. Enzymatic Degradation of Multiple Major Mycotoxins by Dye-Decolorizing Peroxidase from *Bacillus subtilis*. *Toxins (Basel)*. **13**, 429. https://doi.org/10.3390/toxins13060429 (2021).
35. Qing, H. et al. *Bacillus subtilis* ANSB168 Producing D-alanyl-D-alanine Carboxypeptidase Could Alleviate the Immune Injury and Inflammation Induced by Ochratoxin A. *Int. J. Mol. Sci.* **22**, 12059. https://doi.org/10.3390/ijms222112059 (2021).
36. Qinghua, W., Vlastimil, D., Kami, K. & Zonghui, Y. Trichothecenes: Structure-Toxic Activity Relationships. *Curr. Drug Metab.* **14**, 641–660. https://doi.org/10.2174/1389200211314060002 (2013).
37. Righetti, L. et al. Plant biotransformation of T2 and HT2 toxin in cultured organs of *Triticum durum* Desf. *Sci. Rep.* **9**, 14320. https://doi.org/10.1038/s41598-019-50786-w (2019).
38. Rocha, O., Ansari, K. & Doohan, F. M. Effects of trichothecene mycotoxins on eukaryotic cells: A review. *Food Addit. Contam.* **22**, 369–378. https://doi.org/10.1080/02652030500058403 (2005).
39. Samara, A., Yagen, B., Agranat, I., Rachmilewitz, E. A. & Fibach, E. Induction of differentiation in human myeloid leukemic cells by T-2 toxin and other trichothecenes. *Toxicol. Appl. Pharmacol.* **89**, 418–428. https://doi.org/10.1016/0041-008X(87)90161-X (1987).
40. Savard, M. E., Blackwell, B. A. & Greenhalgh, R. An ^{1}H nuclear magnetic resonance study of derivatives of 3-hydroxy-12,13-epoxytrichothec-9-enes. *Can. J. Chem.* **65**, 2254–2262. https://doi.org/10.1139/v87-376 (1987).
41. Sun, F. et al. CotA laccase from *Bacillus licheniformis* ZOM-1 effectively degrades zearalenone, aflatoxin B_1 and alternariol. *Food Control*. **145**, 109472. https://doi.org/10.1016/j.foodcont.2022.109472 (2023).
42. Sun, Y. X. et al. Toxicokinetics of T-2 toxin and its major metabolites in broiler chickens after intravenous and oral administration. *J. Vet. Pharmacol. Ther.* **38**, 80–85. https://doi.org/10.1111/jvp.12142 (2015).
43. Ueno, Y. et al. Metabolism of T-2 toxin in *Curtobacterium* sp. strain 114-2. *Appl. Environ. Microbiol.* **46**, 120–127. https://doi.org/10.1128/aem.46.1.120-127.1983 (1983).
44. van Meerloo, J., Kaspers, G. J. L. & Cloos, J. Cell Sensitivity Assays: The MTT Assay. In: (ed Cree, I. A.) Cancer Cell Culture: Methods and Protocols, 2 edn. Humana, Totowa, New Jersey, 237–245. https://doi.org/10.1007/978-1-61779-080-5_20 (2011).

45. Vanhoutte, I., Audenaert, K. & De Gelder, L. Biodegradation of Mycotoxins: Tales from Known and Unexplored Worlds. *Front. Microbiol.* 7. https://doi.org/10.3389/fmicb.2016.00561 (2016).
46. Wang, W. et al. The Ribosome-Binding Mode of Trichothecene Mycotoxins Rationalizes Their Structure—Activity Relationships. *Int. J. Mol. Sci.* **22**, 1604. https://doi.org/10.3390/ijms22041604 (2021).
47. Yang, C-M., Mahror, N., Li, S-J., Liu, L. & Cheng, L-H. Biodegradation of T-2 Toxin by a Dominant Microbial Consortium Isolated From Chinese Yeast Ball. eFood, **6**:e70047. (2025). https://doi.org/10.1002/efd2.70047
48. Yang, S. et al. Metabolism of T–2 Toxin in Farm Animals and Human In Vitro and in Chickens In Vivo Using Ultra High-Performance Liquid Chromatography- Quadrupole/Time-of-Flight Hybrid Mass Spectrometry Along with Online Hydrogen/Deuterium Exchange Technique. J Agric Food Chem, 65:7217–7227. (2017). https://doi.org/10.1021/acs.jafc.7b02575
49. Yang, X. et al. Spermatogenesis disorder caused by T-2 toxin is associated with germ cell apoptosis mediated by oxidative stress. *Environ. Pollut*. **251**, 372–379. https://doi.org/10.1016/j.envpol.2019.05.023 (2019).
50. Yao, J., Ouyang, B., Xu, W., Xie, Y. & Mu, W. An overview of the physical, chemical and biological strategies for the removal of emerging mycotoxins: Recent advances and future perspectives. *Food Control*. **181**, 111700. https://doi.org/10.1016/j.foodcont.2025.111700 (2026).
51. Zhang, J., Liu, X., Su, Y. & Li, T. An update on T2-toxins: metabolism, immunotoxicity mechanism and human assessment exposure of intestinal microbiota. *Heliyon* **8**, e10012. https://doi.org/10.1016/j.heliyon.2022.e10012 (2022).
52. Zhang, X., Wang, Y., Velkov, T., Tang, S. & Dai, C. T-2 toxin-induced toxicity in neuroblastoma-2a cells involves the generation of reactive oxygen, mitochondrial dysfunction and inhibition of Nrf2/HO-1 pathway. *Food Chem. Toxicol.* **114**, 88–97. https://doi.org/10.1016/j.fct.2018.02.010 (2018).
53. Zhang, Z., Schwartz, S., Wagner, L. & Miller, W. A greedy algorithm for aligning DNA sequences. *J. Comput. Biol.* **7**, 203–214. https://doi.org/10.1089/10665270050081478 (2000).

Figures

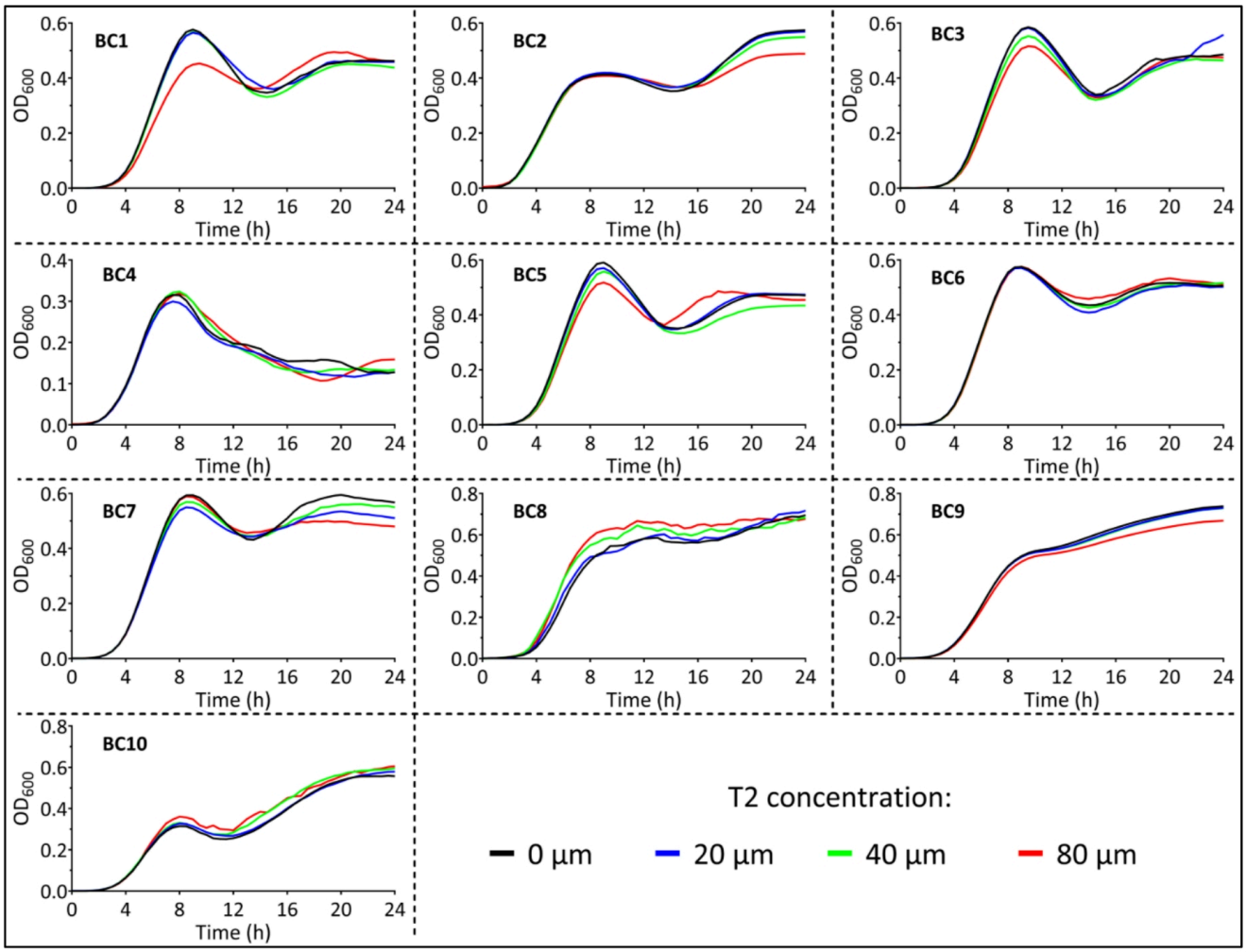


Figure 1

Growth curves of ten Bacillus cultures (BC1 – 10) over 24 h at 37 °C in TSB medium containing different concentrations of T-2

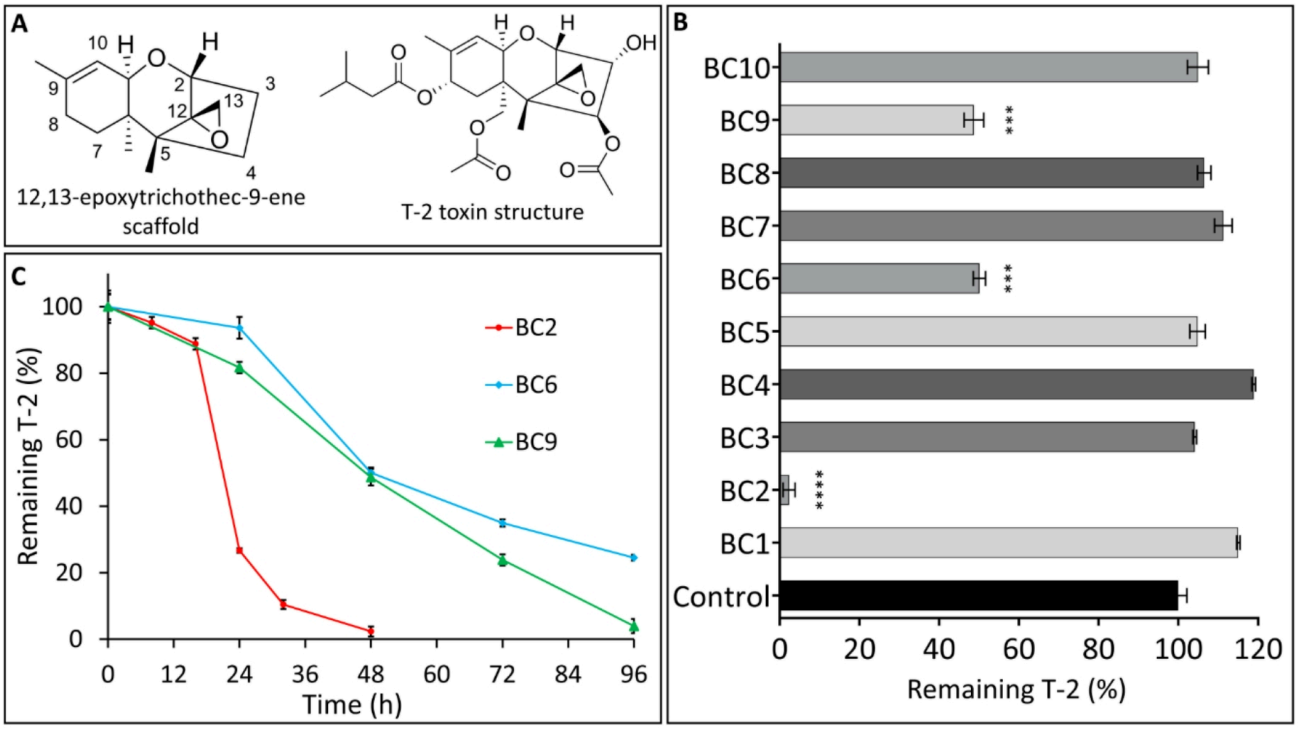


Figure 2

Summary of T-2 removal results for BC1 – 10

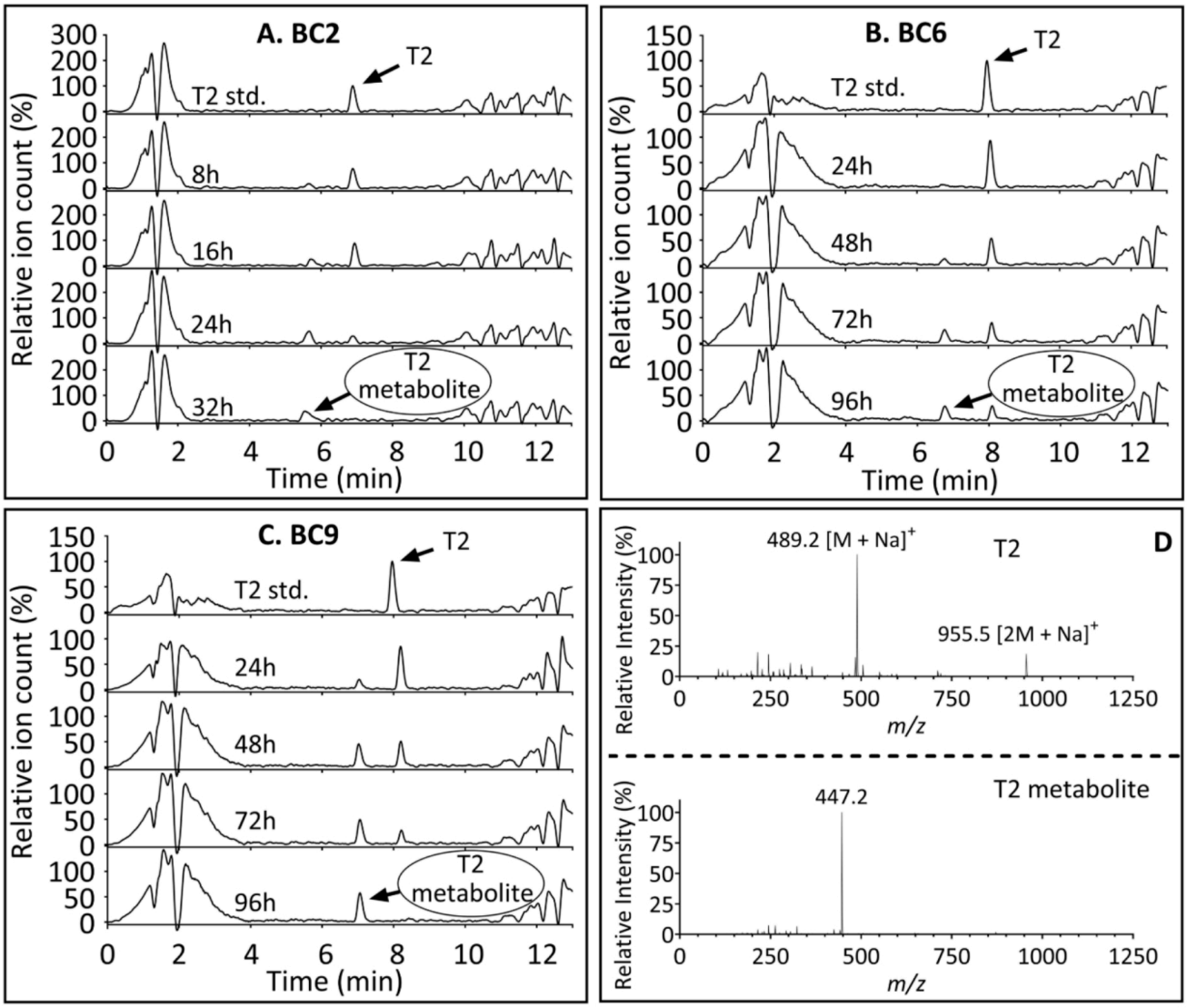


Figure 3

Kinetic monitoring of T-2 biotransformation for BC2, BC6, and BC9

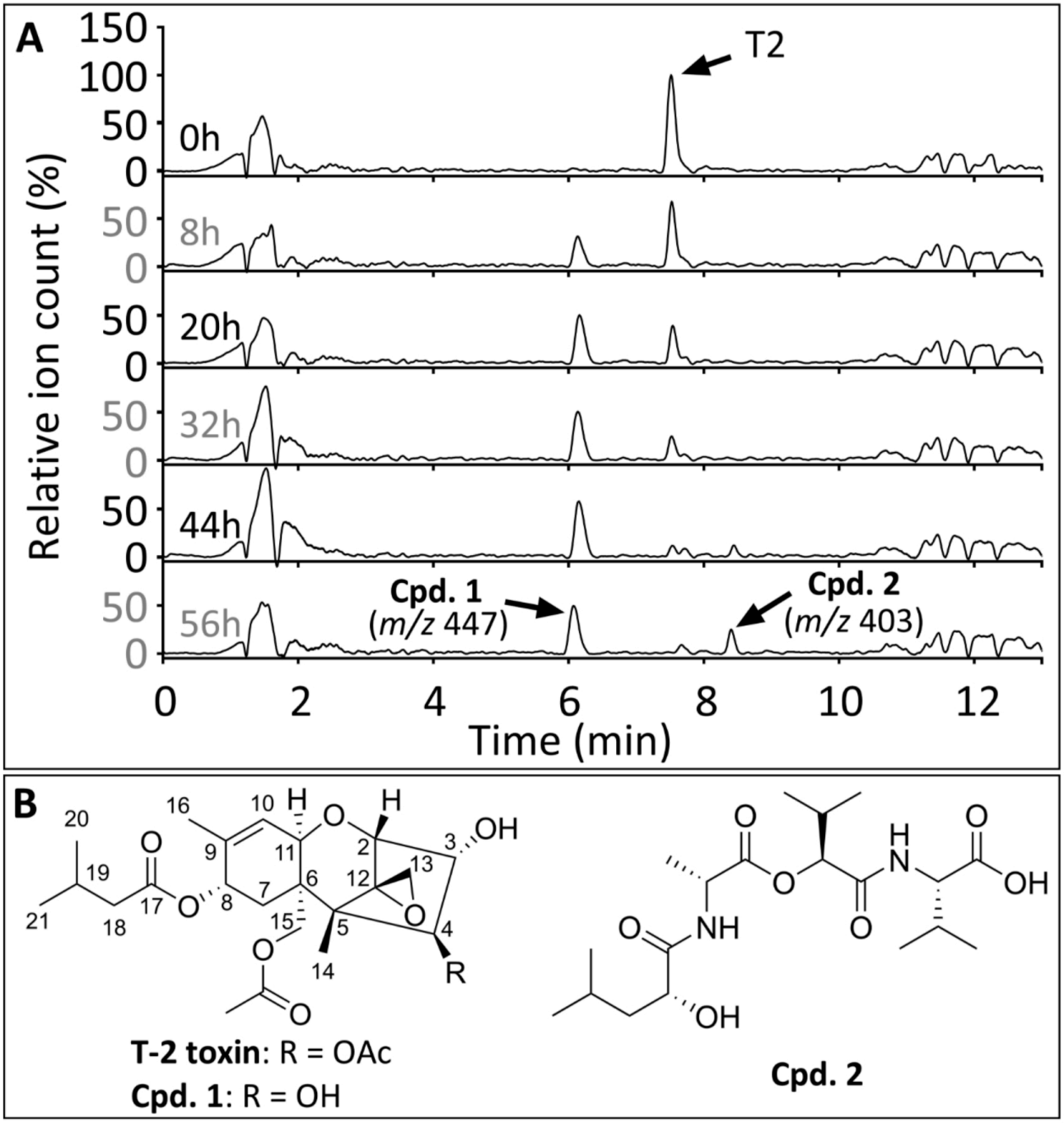


Figure 4

Kinetic monitoring of T-2 metabolism in large-scale culture of BC2

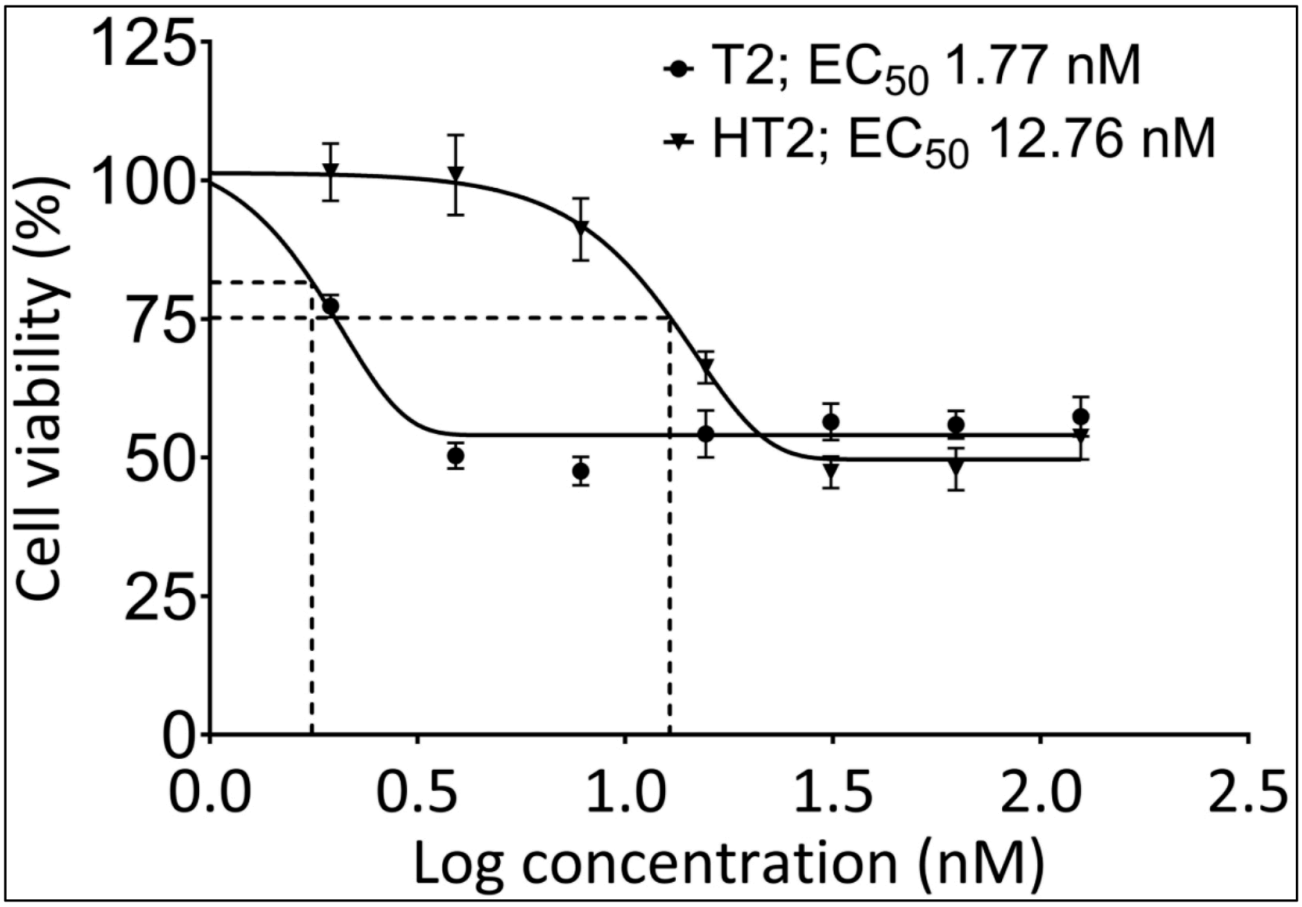


Figure 5

Cell viability study of HEK293T cells treated with T-2 and HT-2

Supplementary Files

This is a list of supplementary files associated with this preprint. Click to download.

- SupplementaryInformation.docx